

See discussions, stats, and author profiles for this publication at: <https://www.researchgate.net/publication/280059488>

# Galectin-3 Binding Protein and Galectin-1 Interaction in Breast Cancer Cell Aggregation and Metastasis

ARTICLE *in* JOURNAL OF THE AMERICAN CHEMICAL SOCIETY · JULY 2015

Impact Factor: 12.11 · DOI: 10.1021/jacs.5b04744 · Source: PubMed

---

READS

78

## 7 AUTHORS, INCLUDING:



Chein-Hung Chen

Academia Sinica

24 PUBLICATIONS 395 CITATIONS

[SEE PROFILE](#)



Tsui-Ling Hsu

Academia Sinica

39 PUBLICATIONS 1,657 CITATIONS

[SEE PROFILE](#)

# **Galectin-3 binding protein and galectin-1 interaction in breast cancer cell aggregation and metastasis**

Tzu-Wen Lin<sup>†,‡</sup>, Hui-Tzu Chang<sup>†,§,¶</sup>, Chein-Hung Chen<sup>†</sup>, Chung-Hsuan Chen<sup>†</sup>,  
Sheng-Wei Lin<sup>‡</sup>, Tsui-Ling Hsu<sup>†</sup> and Chi-Huey Wong<sup>†\*</sup>

<sup>†</sup>Genomics Research Center, Academia Sinica, 128 Academia Road, Section 2,  
Nankang, Taipei 115, Taiwan

<sup>§</sup>Institute of Biochemistry and Molecular Biology, National Yang-Ming University,  
Taipei 112, Taiwan

<sup>‡</sup>Institute of Biological Chemistry, Academia Sinica, 128 Academia Road, Section 2,  
Nankang, Taipei 115, Taiwan

\*Address correspondence to:

Chi-Huey Wong, Genomics Research Center, Academia Sinica,  
128 Academia Road Section 2, Taipei 115, Taiwan. Tel: 886-2-2789-7400; Fax: 886-  
2-2785-3852; Email: chwong@gate.sinica.edu.tw.

## **Abstract**

Galectin-3 binding protein (Gal-3BP) is a large hyperglycosylated protein that acts as a ligand for several galectins through glycan-dependent interactions. Gal-3BP can induce galectin-mediated tumor cell aggregation to increase the survival of cancer cells in the bloodstream during the metastatic process. However, the galectin interacting with Gal-3BP and its binding specificity has not been identified and structurally elucidated, mainly due to the limitation of mass spectrometry in glycan sequencing. To understand the role of Gal-3BP, we here used liquid chromatography-mass spectrometry combined with specific exoglycosidase reactions to determine the sequences of *N*-glycans on Gal-3BP from MCF-7 and MDA-MB-231 cells, especially the sequences with terminal sialylation and fucosylation, and addition of LacNAc repeat structures. The *N*-glycans from both strains are complex type with terminal  $\alpha$ 2,3-sialidic acid and core fucose linkages, with additional  $\alpha$ 1,2- and  $\alpha$ 1,3 fucose linkages found in MCF-7 cells. Compared with that from MCF-7, the Gal-3BP from MDA-MB-231 cells had fewer tetra-antennary structures, only  $\alpha$ 1,6-linked core fucoses, and more LacNAc repeat structures; the MDA-MB-231 cells had no surface galectin-3 but used surface galectin-1 for interaction with Gal-3BP to form large oligomers and cell aggregates. This study elucidates the specificity of Gal-3BP interacting with galectin-1 and the role of Gal-3BP in cancer cell aggregation and metastasis.

## **Introduction**

Glycoconjugates on the cell surface play important roles in a variety of biological functions. Various glycan structures are present in different cell types and at different developmental and differentiation stages, and are modified in many pathological states including cancers<sup>1</sup>. Aberrant glycosylation is frequently observed in various tumor cells and some glycan biomarkers have been utilized for detection of cancer (e.g., CA19-9 and CA-125), and development of vaccines<sup>2</sup>. Glycan changes in glycoproteins that correlate with tumor progression include aberrant branching of *N*-linked glycans, terminal sialylation and fucosylation, expression of sialylated Lewis structures, truncation of *O*-linked glycans and expression of the poly-*N*-acetyllactosamine (poly-LacNAc) structure<sup>3</sup>. Altered oligosaccharides on glycoproteins can affect glycoprotein folding and stability, and interfere with carbohydrate-carbohydrate, carbohydrate-protein, and glycoprotein-glycoprotein interactions, and as a result, regulate many physiological and pathological events. Therefore, specific glycan structures have been suggested to be signatures of certain disease states such as cancer metastasis<sup>4</sup>.

Gal-3 binding protein (Gal-3BP), also known as Mac-2 binding protein (Mac-2BP) or tumor-associated antigen 90K (TAA90K), is a glycoprotein without a transmembrane domain. Gal-3BP is expressed in various cell types, including hematopoietic cells and glandular or mucosal epithelia, and is present at high levels in the serum and other biological fluids of patients<sup>5, 6</sup> with pancreatic, breast, or lung cancer, and patients with AIDS, hepatitis, and autoimmune diseases<sup>7-10</sup>. It has been reported that breast cancer patients with serum Gal-3BP exceeding 11 µg/ml have poor prognosis and metastasis<sup>11</sup>; Gal-3BP is therefore considered to be a tumor-associated antigen of breast cancer.

Gal-3BP is a highly glycosylated protein with seven *N*-linked glycosylation sites. Gal-3BP can self-assemble to form large homo-oligomers in a linear or ring-like shape, and ring-ring association is also observed<sup>12</sup>. These multimeric forms of Gal-3BP are believed to increase the interaction with multiple targets, including galectins-1, -3, -7, and the extracellular matrix (ECM, including collagen IV, V and VI, fibronectin, laminin-1, -5 and -10, and  $\beta$ 1-integrin). Recently, Gal-3BP was also demonstrated to bind other lectins on immune cells, including dendritic cell-specific intercellular adhesion molecule 3-grabbing non-integrin (DC-SIGN) and E-selectin<sup>13</sup>,<sup>14</sup>, and the interaction of Gal-3BP and Gal-3 has been confirmed to be carbohydrate-dependent<sup>15, 16</sup>. Although the biological functions of Gal-3BP remain unclear, the induction of homotypic cell aggregation by Gal-3BP<sup>16</sup> is considered to facilitate tumor metastasis by preventing anoikis of metastatic cells in the blood stream<sup>17</sup>. Moreover, the interaction of Gal-3BP and ECM may also relate to the adhesiveness of tumor cells *in situ*<sup>18</sup>.

As glycosylation plays an important role in modulating the behavior of Gal-3BP in cancer progression, we decided to first identify the galectin that interacts with Gal-3BP and the sequences of *N*-linked glycans on the Gal-3BP from different breast cancer cell lines to investigate their structures and ability to enhance tumor aggressiveness. The glycan sequences were determined by liquid chromatography-mass spectrometry (LC-MS) combined with exoglycosidase treatment and lectin-based ELISA to overcome the limitation of LC-MS method alone. Gal-3BP from MDA-MB-231, an aggressive breast cancer cell line, induced a higher level of homotypic cell aggregation than the Gal-3BP from MCF-7. We also observed that the Gal-3BP from MDA-MB-231 formed a larger homo-oligomer. Understanding the differences of Gal-3BPs from MDA-MB-231 and MCF-7 cells in terms of *N*-glycans sequences and their spatial arrangement, as well as the specificity of

Gal-3BP-lectin interaction will provide valuable information for use to elucidate the role of Gal-3BP in cancer cell aggregation and metastasis.

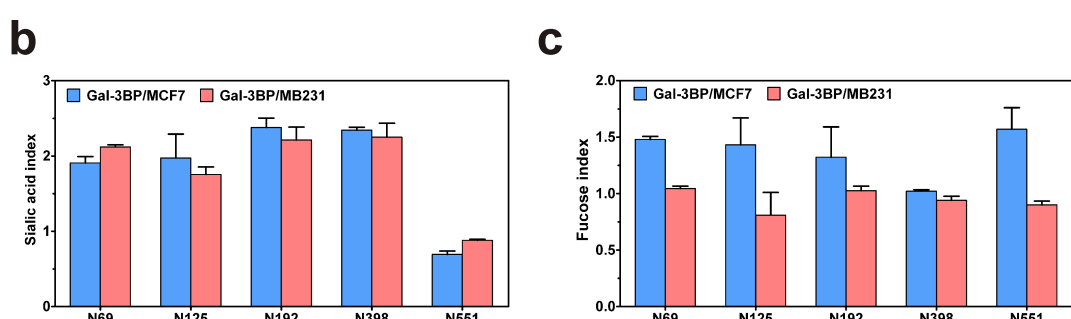
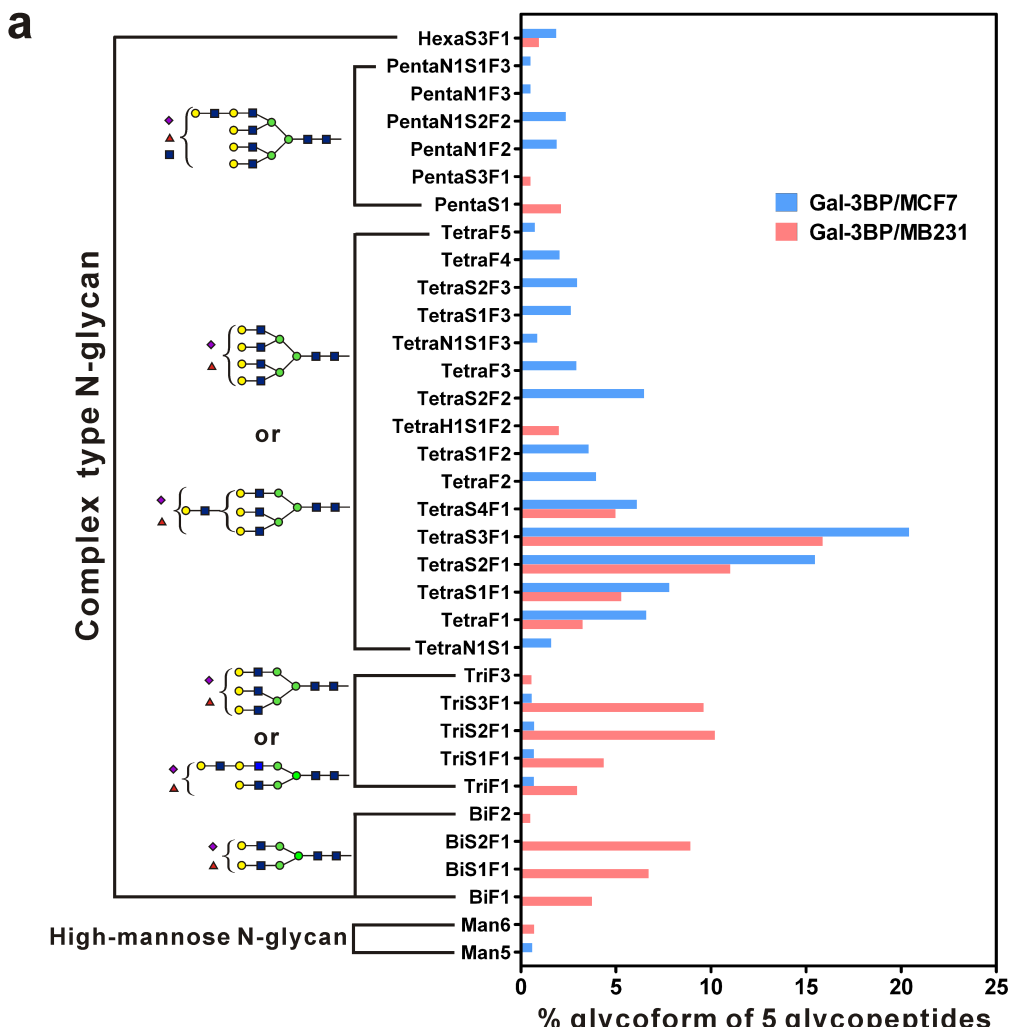
## Results and discussion

It has been proposed that Gal-3BP is a breast cancer-specific antigen<sup>19</sup>. To understand how the glycans on Gal-3BP affect the behavior of breast cancer cells, we overexpressed and purified Gal-3BP in two breast cancer cell lines, MCF-7 (mild) and MDA-MB-231 (aggressive). After PNGaseF digestion to remove the *N*-linked glycans, the molecular weight of each species shifted from ~90 kDa to 65 kDa as expected (65,331 Da as calculated based its amino acid sequence) (Supplementary information, Fig. S1). We then immobilized and compared the Gal-3BPs from MCF-7 and MDA-MB-231 for their binding to Gal-3 in microtiter plates, and found that Gal-3 did interact with Gal-3BP (Fig. S2a). The binding affinity of Gal-3BP/MB231 was significantly higher than Gal-3BP/MCF7 at low concentrations of Gal-3, and a similar trend was also observed in the binding of endogenous Gal-3BP from MCF-7 and MDA-MB-231 toward Gal-3, indicating that the overexpressed Flag-tagged Gal-3BP could represent native Gal-3BP (Fig. S2b). This result suggested that Gal-3BP/MB231 with higher affinity for Gal-3 was due to the *N*-glycans on Gal-3BPs, since the recombinant Gal-3BP was produced by the same expression construct, and the nucleotide sequences of endogenous Gal-3BP in both MCF-7 and MDA-MB-231 were identical (data not shown).

In order to link the glycans specifically expressed on Gal-3BP of breast cancer cells with their function, we next performed site-specific glycoprofiling of Gal-3BPs by LC-MS/MS. This method is based on matching the experimental masses with the predicted masses of tryptic peptide fragments and the glycans from the CFG carbohydrate database, and confirmed the existence of ionized glycan fragments in MS/MS spectra. The glycoforms of individual glycopeptides were quantified and calculated for their proportions in all the glycoforms observed on a specific glycopeptide. Gal-3BP was observed to have *N*-glycans on the expected glycosylation

sites, but there was no *O*-glycans detected. Five out of seven expected *N*-glycosylation sites were consistently identified in tryptic glycopeptides, including Asn (N) 69, N125, N192, N398 and N551 (Fig. 1a). The other two glycopeptides with N362 and N580 respectively, were detected with very weak signal and therefore were not listed. Most *N*-linked glycans of Gal-3BPs from these two cell lines were complex-type glycans containing sialic acids and fucoses. High-mannose or hybrid-type glycans were only found at low percentages in the glycopeptide of N551. The size of complex-type glycans and the fucosylation status were very different in Gal-3BP/MCF7 and Gal-3BP/MB231: bigger *N*-linked glycans were observed in Gal-3BP/MCF7 (MCF7, tetra-antennary 85%; MB231, bi-antennary 20%, tri-antennary 28% and tetra-antennary 43%). The level of sialylation and fucosylation at each glycosylation site was calculated as sialic and fucose indexes (Fig. 1b and 1c) and compared. The results indicated that the levels of sialylation on these two Gal-3BPs were similar, with a lower sialylation on N551. However, the *N*-linked glycans in Gal-3BP/MB231 had fewer branches and therefore fewer terminal galactoses compared to Gal-3BP/MCF7. There was more fucosylation in Gal-3BP/MCF7, and most *N*-linked glycans (~90%) on Gal-3BP/MB231 carried only one fucose. Among these five glycosylation sites, N398 was less fucosylated and more sialylated, and N551 was less sialylated and more fucosylated, reflecting a pattern of site-specific glycosylation on Gal-3BP. The glycoform data from MS analysis was consistent with lectin-based ELISA. Six lectins were used to detect the binding with Gal-3BPs (Fig. S3): Gal-3BP/MCF7 showed higher PHA-L (for tri- or tetra-antennary *N*-linked glycans) and UEA-I (for  $\alpha$ 1,2-linked fucose) binding intensities, and Gal-3BP/MB231 showed higher MAL-II, SNA, and LEL binding intensities. Therefore, the glycoforms of Gal-3BP/MCF7 contained more tri- or tetra-antennary *N*-linked glycans and  $\alpha$ 1,2-linked fucoses, while Gal-3BP/MB231 had

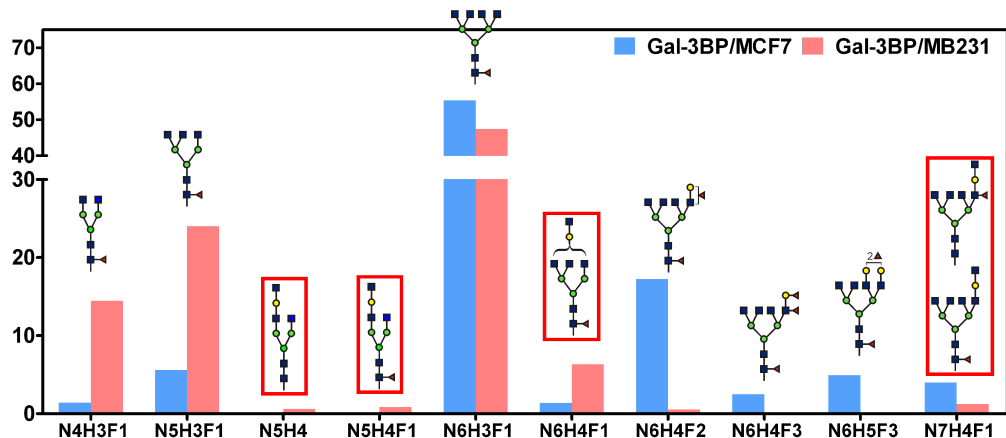
smaller *N*-linked glycans, and had more poly-LacNAc structures.



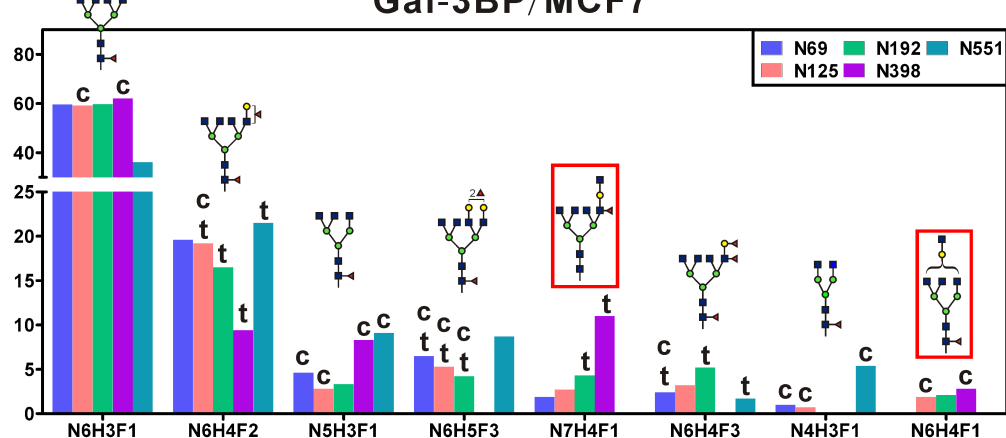
**Figure 1. Glycoform profiling of Gal-3BP.** (a) Glycoforms of Gal-3BP/MCF7 and Gal-3BP/MB231. (b & c) Site-specific sialylation (b) and fucosylation (c). Sialic acid and fucose indexes were calculated based on the following equation:  $\Sigma(\% \text{ of the glycan with sialic acid/fucose} \times \text{the number of the sialic acid/fucose annotated on the site})$

glycan). Man, high mannose; Bi/Tri/Tetra/Penta/Hexa, bi-/tri-/tetra-/penta-/hexa-antennary; F, fucose; S, sialic acid; N, *N*-acetylhexosamine; H, hexose. Symbols for monosaccharides: fucose, triangle; *N*-acetylglucosamine, blue square; galactose, yellow circle; mannose, green circle; *N*-acetylneuraminic acid, diamond.

Poly-LacNAc is a high affinity ligand for Gal-3. In the lectin assay, we discovered that Gal-3BP could be recognized by LEL, which binds to poly-LacNAc. The number of poly-LacNAc moieties on Gal-3BP may be an important key factor affecting the affinity for Gal-3. Here, we have designed a method to identify poly-LacNAc on Gal-3BP glycopeptides using  $\beta$ 1,3/4-galactosidase to differentiate from the multibranched LacNAc structures. Before enzyme digestion, we chemically removed the terminal sialic acid to expose terminal galactose residues, then used  $\beta$ 1,3/4-galactosidase to remove the terminal galactose. If the *N*-glycans contain poly-LacNAc residues, the outer galactose is removed by the enzyme but the exposed GlcNAc can protect the inner galactose from further cleavage. The terminal fucoses, including the  $\alpha$ 1,2-,  $\alpha$ 1,3- or  $\alpha$ 1,4-fucose linkages also resist  $\beta$ 1,3/4-galactosidase digestion. In addition, we checked the MS/MS spectrum to detect the presence of 512.2 oxonium ion as an indicator of the terminal fucose signal and peptide+HexNAc+Fuc ion as a core fucose signal (Table S1). The results showed that major *N*-glycans with one fucose have no 512.2 oxonium ion signal, indicating core fucosylation. Therefore, the *N*-glycans with extra hexose residues (over three core mannoses) without outer fucose residues could be derived from the *N*-glycans containing the poly-LacNAc substructure. Degalactosylated glycopeptides were analyzed using LC-MS/MS to observe glycan compositions (Fig. 2) and the location of fucose. Only four glycoforms, N5H4S0F0, N5H4S0F1, N6H4S0F1 and N7H4S0F1 corresponded to the *N*-glycans with poly-LacNAc.

**a****b**

### Gal-3BP/MCF7

**c**

### Gal-3BP/MB231

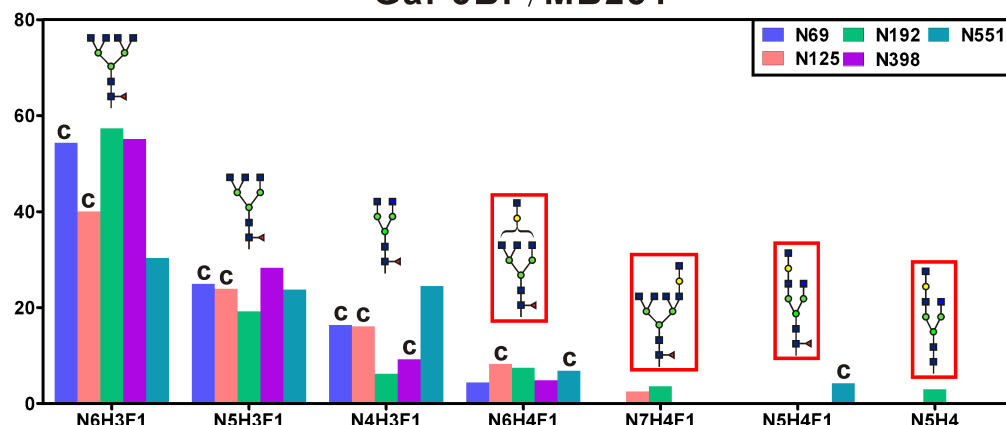


**Figure 2. Degalactosylation of Gal-3BP for poly-LacNAc structure determination.**

(a) Degalactosylated glycoforms of Gal-3BP/MCF7 and Gal-3BP/MB231. (b &c) Site-specific glycoforms of Gal-3BP/MCF7 (b) and Gal-3BP/MB231(c). Possible glycan structures are drawn on top of each bar. The glycoforms with oxonium ions,

$m/z = 512.2$ , in MS/MS spectra, are labeled with **t** (terminal fucose). The glycoforms with ions corresponding to the mass of peptide-HexNAc-Fuc fragments in the MS/MS spectra are labeled with **c** (core fucose). The glycoforms with poly-LacNAc structure are highlighted with red boxes.

We calculated the sum of these four glycoforms in every *N* glycosite on the Gal-3BPs (Table 1). Gal-3BP/MB231 had higher glycoforms with poly-LacNAc (9.01%) than MCF-7 (5.34%). Furthermore, the distribution of *N*-glycans with poly-LacNAc on the glycosites was different in these two Gal-3BPs; Gal-3BP/MB231 had three glycosites (N125, 192 and 551) over 10% but Gal-3BP/MCF7 had only one (N398), and the major glycoform on Gal-3BP/MB231 was from N6H4S0F1 and that on Gal-3BP/MCF7 was from N7H4S0F1. This result indicated that the higher binding ability of Gal-3BP/MB231 for Gal-3 could come from the contribution of the poly-LacNAc substructure.

<i>N</i> -glycosite	Gal-3BP from MCF-7	Gal-3BP from MDA-MB-231
N69	1.94%	4.40%
N125	4.58%	10.75%
N192	6.42%	14.43%
N398	13.76%	4.81%
N551	0.00%	11.07%
Average	5.34%	9.01%

**Table 1. Potential *N*-glycans with poly-LacNAc in the *N*-glycosylation site**

Through degalactosylated glycopeptide profiling, we also discovered and determined the major glycoforms of Gal-3BP/MCF7 (Fig. 2b) and Gal-3BP/MB231

(Fig. 2c). After galactosidase digestion, most *N*-glycans of Gal-3BP/MB231 only retained three hexose residues from the core structure and had only one fucose. Based on the characteristics of enzyme digestion and MS/MS spectra of glycopeptides, we believe that the location of the fucose residue was on the *N*-glycan core (core fucosylation). On the other hand, there was almost no terminal fucose signal in the MS/MS spectra of Gal-3BP/ MB231 glycopeptides. Therefore, the three major glycoforms of Gal-3BP/MB231 were bi- (14.5%), tri- (24%) and tetra-antennary (47.4%) *N*-glycans with a core fucose and several sialic acids. The major degalactosylated glycoform of Gal-3BP/MCF7 was N6H3S0F1 (~50%) derived from a tetra-antennary *N*-glycan with core fucose. The other glycoforms also had six HexNAc residues and multiple fucose residues, so we concluded that the major glycoform of Gal-3BP/MCF7 was the tetra-antennary structure with a core fucose and outer arm fucose and sialic acids. These results were also confirmed by the glycopeptide profiling and lectin assay.

The other specific exoglycosidases, including  $\alpha$ 2,3-sialidase,  $\alpha$ 1,2- and  $\alpha$ 1,3/4-fucosidase, are useful for determining the terminal sialic acid and fucose linkages, which are difficult to obtain using mass spectra only. We also compared the glycopeptide profiling of Gal-3BP before and after exoglycosidase digestion. First, we used  $\alpha$ 2,3-sialidase to remove the  $\alpha$ 2,3-linkage sialic acid specifically from the tryptic Gal-3BP glycopeptides (Fig. S4a). The result showed that most sialic acid (over 95%) was removed by this enzyme, indicating that the major sialylation in these two Gal-3BPs was the  $\alpha$ 2,3-linkage. Second,  $\alpha$ 1,2- and  $\alpha$ 1,3/4-fucosidase can release terminal  $\alpha$ 1,2-fucose and subterminal  $\alpha$ 1,3/4-fucose, respectively. Before the treatment with these two enzymes, we also removed the terminal sialic acid to simplify the glycoforms and improve signal intensity. According to the previous result, the *N*-glycans on Gal-3BP/MB231 usually carry only one fucose and the fucose is

located in the inner *N*-glycan (core fucose) and is not removed by these two fucosidases. Gal-3BP/MCF7 has many multiple fucosylated glycoforms and was thus performed using fucosidase digestion (Fig. S4b). After  $\alpha$ 1,2-fucosidase treatment, we observed a small increase in mono-fucosylated *N*-glycans and a decrease in *N*-glycans with 2-5 fucose residues. In addition, this digestion only occurred at the N69, 125 and 192 sites with the fucosylation level at the N398 and N551 sites remaining unchanged. The other fucosidase,  $\alpha$ 1,3/4-fucosidase, could reduce the size of *N*-glycans by 2-5 fucoses to about 50% at every *N*-glycosylation site. Therefore,  $\alpha$ 1,2-fucosylation in Gal-3BP/MCF7 is less than  $\alpha$ 1,3-fucosylation, but is site-specific. These two fucosidases cannot remove all fucose residues in the *N*-glycans (as the *N*-glycans without fucose did not increase) and this result also indicates that most *N*-glycans in MCF-7 cells have a core fucose.

In summary, the *N*-glycans of Gal-3BP/MCF7 were tetraantennary *N*-glycans with terminal  $\alpha$ 2,3-sialic acids, and terminal fucoses, and about 5% contained the poly-LacNAc substructure. The *N*-glycans of Gal-3BP/MB231 contained mixtures of bi-, tri- and tetra-antennary *N*-glycans with 2-3 terminal  $\alpha$ 2,3-sialic acids and a core fucose; and about 9% of the glycans contained the poly-LacNAc substructure.

Gal-3BP functions in the induction of homotypic cell aggregation, and the mechanism is considered to proceed through Gal-mediated carbohydrate-dependent interaction. In previous studies, Gal-3BPs showed different binding affinities for Gal-3. We therefore performed the cell aggregation assay to compare the activity (Fig. 3). Compared to Gal-3BP/MCF7, Gal-3BP/MB231 could induce more aggregates of MDA-MB-231 cells. Moreover, we also observed that the ratio of larger aggregates (over 10 cells) induced by Gal-3BP/MB231 was obviously higher than that of Gal-3BP/MCF7. In the microscopic images, huge cell aggregates were observed after treatment with Gal-3BP, and the added Gal-3BP was found to be located at the

cell-cell contact region as shown by the anti-Gal-3BP antibody staining (Fig. 3c). Because the aggregation of MDA-MB-231 cells induced by Gal-3BP was also inhibited by lactose but not sucrose (Fig. 3b), it is believed to be a carbohydrate-dependent interaction.

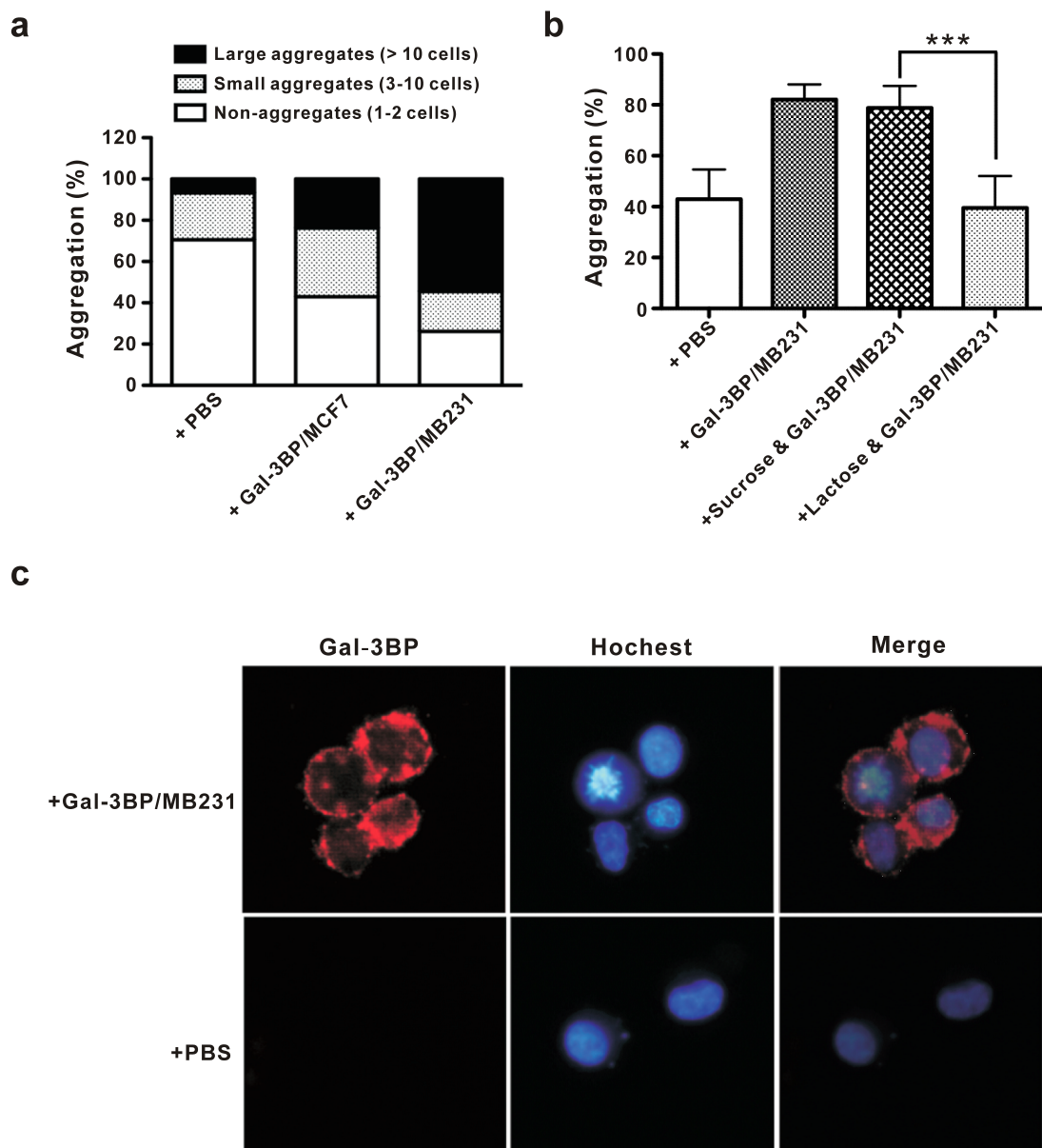


**Figure 3. Gal-3BP induced carbohydrate-dependent cell aggregation in breast cancer cells.** (a) Induction of MDA-MB-231 aggregation by Gal-3BP/MCF7 or Gal-3BP/MB231. Gal-3BP (5  $\mu$ g/ml) was used to treat cells for 1 h, and the degree of cell aggregation was quantitated by Image J. (b) Homotypic MDA-MB-231

aggregation was inhibited by lactose. Lactose (10 mM) or sucrose (10 mM) was added together with Gal-3BP and degrees of cell aggregation were quantified. Results are shown as mean  $\pm$  SD ( $n = 5$ ). \*\*\*,  $P < 0.001$  compared with sucrose treatment by Student t test. (c) Gal-3BP was detected on the cell surface and at the regions of cell-cell contact under fluorescence microscopy. MDA-MB-231 cells were subjected to aggregation assay and then stained with anti-Gal-3BP pAb (red) or Hoechst 33342 (nuclear stain, shown in blue color). The cells incubated with PBS were stained as a negative control.

In order to understand whether MDA-MB-231 cell aggregation was galectin-dependent, we investigated the expression profiles of all the known human Gals in MDA-MB-231 cells. By examining the mRNA expression via Q-PCR and their expression levels on the cell surface by flow cytometry (Fig. 4), we found that MDA-MB-231 cells could express Gal-1, 3, 8 and 9 mRNA. However, it is interesting that only Gal-1 and 8, but not Gal-3, were detected on the cell surface of MDA-MB-231 (Fig. 4b), while the expression of Gal-3 was detected on MCF-7 (Fig. 4b, inset of Gal-3 staining), indicating that anti-Gal-3 could detect Gal-3 on the cell surface. This result suggested that the aggregation of MDA-MB-231 induced by Gal-3BP was not mediated by Gal-3, and could possibly be mediated by Gal-1 or 8. Interaction of Gal-1 and Gal-3BP was reported to be involved in homotypic cell aggregation in human melanoma A375 cell line. To explore the relative contribution of Gal-1 to MDA-MB-231 cell aggregation, Gal-1-deficient cells were established by two kinds of Gal-1 siRNA (siGal1#1 and siGal1#2). The mRNA and cell surface expression of Gal-1 in the two Gal-1-deficient cell lines were significantly reduced compared to parental and control cells (Fig. S5). We performed cell aggregation assay with or without additional Gal-3BP (Fig. 4c). Gal-1-deficient cells had less cell

aggregation induced by Gal-3BP, and the percentage of large aggregates (siGal1#1: 43%, siGal1#2: 40%) was lower compared to control cells. This result suggested that Gal-3BPs interact with Gal-1 on the cell surface to induce MDA-MB-231 cell aggregation with large cell aggregates. To analyze the interaction between Gal-1 and Gal-3BPs, we performed surface plasmon resonance (SPR). The sensorgrams revealed that the association and dissociation of Gal-1 to Gal-3BPs was very rapid (Fig. S6). The  $K_D$  values of Gal-3BP/MCF7 and Gal-3BP/MB231 binding to Gal-1 calculated by steady-state analysis were 2.34 and 1.88  $\mu\text{M}$ , respectively, showing that the binding affinities of Gal-1 toward Gal-3BP/MCF7 and Gal-3BP/MB231 were similar (Fig. 4d). Interestingly, the binding of Gal-3BP/MCF7 and Gal-3BP/MB231 to immobilized Gal-1 in ELISA-type binding experiment showed that Gal-3BP/MB231 had a higher binding intensity toward Gal-1 comparing to Gal-3BP/MCF7 (Fig. 4e).

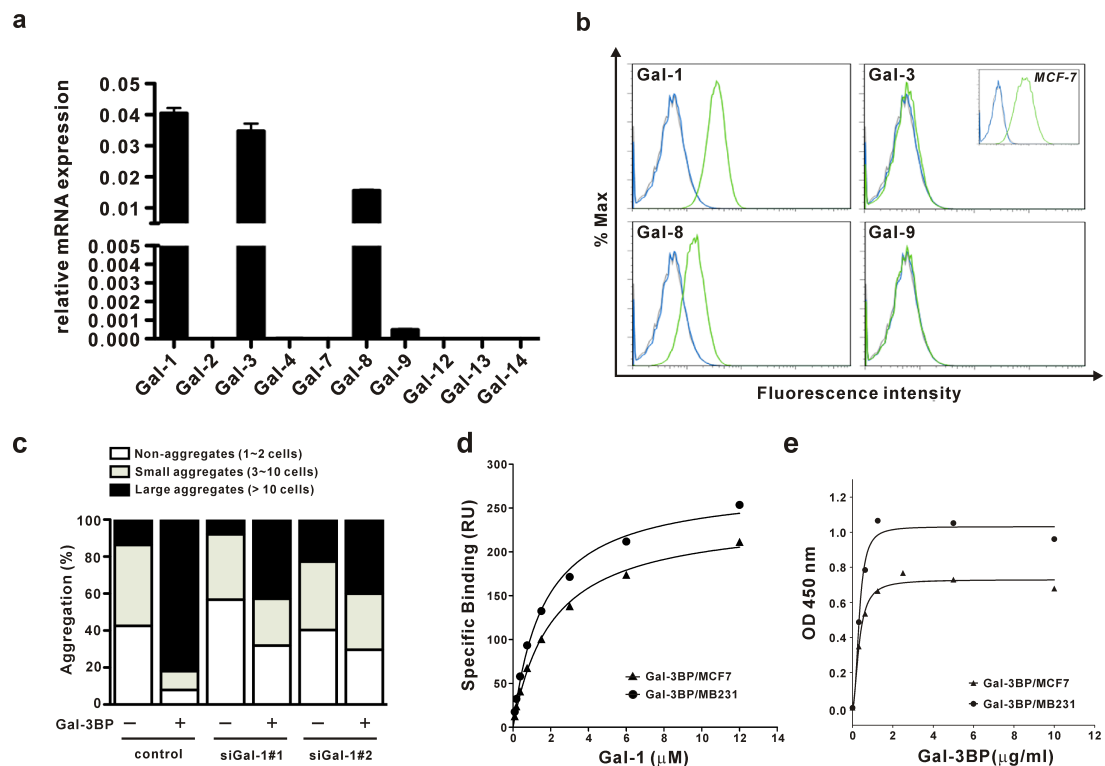


**Figure 4. Expression profiles of galectin (Gal) in breast cancer MDA-MB-231**

**cells and the interaction of Gal-1 and Gal-3BP.** (a) Q-PCR analysis for Gal mRNA expression in MDA-MB-231 cells. The expression of Gal was normalized against the expression level of GAPDH mRNA. (b) Flow-cytometric analysis of galectin expression on MDA-MB-231 cells. Blue histograms, isotype control staining; green histograms, anti-galectin staining. Inset: Flow-cytometric analysis of Gal-3 expression on MCF-7 cells. (c) Aggregation of the cells knocked down with Gal-1 upon treatment of Gal-3BP. MDA-MB-231 cells transfected with negative control or Gal-1 siRNA were incubated in the presence of Gal-3BP/MB231 (10 µg/ml). After 1 h of incubation, the degrees of cell aggregation were quantitated by Image J. (d) SPR-derived steady state affinity for Gal-1 over Gal-3BPs. Gal-3BP/MCF7 and Gal-3BP/MB231 were immobilized on sensor chips and Gal-1 in various concentrations were applied to calculate for  $K_D$ . (e) Binding ability of Gal-3BPs to immobilized Gal-1 in ELISA-type binding assay.

Because of oligomerization, native human Gal-3BPs can self-assemble to form huge macromolecules with ring-like structures. These protein macromolecules contain 10-16 monomers and about 70-116 *N*-glycans on one protein oligomer. A previous study indicated that Gal-3BP oligomers may contribute to the multivalent effect of Gal-3BP, which binds to multiple targets<sup>15</sup>. To validate the oligomerization of the Gal-3BPs, we observed protein oligomers of Gal-3BP/MCF7 and Gal-3BP/MB231 using HPLC SEC-MALLS (Fig. S7). Analysis of the molar mass of these two protein oligomers indicated that Gal-3BP/MB231 could form bigger oligomers (1502 kDa) than Gal-3BP/MCF7 (1138 kDa). Based on the molecular weight of Gal-3BP monomer (~90 kDa), Gal-3BP/MB231 oligomer is composed of 16-17 monomers and Gal-3BP/MCF7 oligomer is composed of 12-13 monomers.

In this study, we investigated the glycosylation changes in breast cancer cells to

understand why the tumor cells show altered glycosylation state during tumorigenesis. We studied the glycosylation profile of a hyperglycosylated glycoprotein, Gal-3BP, which has been suggested to be a breast cancer marker, from two cell lines (MCF-7 and MDA-MB-231) with different metastatic abilities. We used LC-MS/MS to analyze the glycoforms of Gal-3BP glycopeptides site-specifically, and introduced exoglycosidases with linkage specificity to facilitate the determination of detailed glycan structures, including the linkages of terminal sialic acids and fucoses, and the substructures of glycan branching and poly-LacNAc.

The results revealed that Gal-3BP/MB231 had a stronger interaction with Gal-3 than Gal-3BP/MCF7 (Fig. S2) did. Since Gal-3BP interacts with Gal-3 in a carbohydrate-dependent manner, the glycans on Gal-3BP are the major factors that modulate the interaction with Gal-3. It has been reported that a tetraantennary *N*-linked glycan fully capped with sialic acid can also interact with Gal-3, and the binding intensity can be increased up to eight-fold if one poly-LacNAc unit is added<sup>20</sup>. Our glycan profiling results showed that poly-LacNAc was more predominant on Gal-3BP/MB231, indicating that this structure could be the key determinant in binding to Gal-3. Glycan profiling showed that the major glycoforms of Gal-3BPs from both breast cancer cell lines were bi-, tri- and tetra-antennary *N*-linked glycans with sialylation and fucosylation. It has been reported that  $\alpha$ 2,3- and  $\alpha$ 2,6-sialylation and  $\alpha$ 1,3-fucosylation can partially or completely inhibit the binding between Gal-3BP and Gal-3, while  $\alpha$ 1,2-fucosylation has no inhibitory effect on Gal-3BP/Gal-3 interaction<sup>21</sup>. This finding is also supported by our results that showed that removal of the sialic acids on Gal-3BP increased its binding ability to Gal-3 (data not shown).

We also determined the position of fucose by LC-MS/MS. The oxonium ion with m/z = 512.2 (Hex-HexNAc-Fuc) can be used to identify terminal fucosylation. The profile of glycoforms after exo-galactosidase treatment also helps locate terminal fucoses since the enzyme is unable to cleave terminal galactose if the LacNAc unit is fucosylated. However, if the position of the fucose cannot be clearly assigned, especially when there is only one fucose in the whole glycan, it is difficult to locate the position of LacNAc unit in the poly-LacNAc structure or as a branch of the glycan chain. In this case, treatment with  $\beta$ 1,3/4-galactosidase plus  $\alpha$ 1,2- and  $\beta$ 1,3/4-fucosidases can be used to assign the correct glycan structures.

In order to understand the effect of *N*-glycans on Gal-3BPs, we performed an aggregation assay by treating MDA-MB-231 cells with Gal-3BPs. Our result was consistent with reports that the formation of Gal-3BP-induced cell aggregates is a carbohydrate-dependent process, because the aggregation was suppressed in the presence of lactose (Fig. 3b). Aggregation of cancer cells can facilitate metastasis by preventing anoikis of cells, a kind of apoptosis induced by loss of cell anchorage. The imaging data also showed that Gal-3BP/MB231 induced more and larger cell aggregates than Gal-3BP/MCF7. In addition to enable the survival of metastatic cells through anoikis, large cell aggregates also promote cell extravasation when getting to the metastasized sites<sup>22</sup>. Our data suggest that Gal-3BP may influence the behavior of cells through its glycosylation, which contributes to the metastasis of cancer cells.

It is also important to determine the galectins involved in the MDA-MB-231 cell aggregation. We stained the Gal-1, 3, 8 and 9 on the cell surface using flow cytometry (Fig. 4b), and the results indicated that Gal-3 was not expressed on the surface of MDA-MB-231 cells. Knockdown of Gal-1 was found to inhibit the formation of large cell aggregates in MDA-MB-231 cells, indicating that the behavior of Gal-3BP-induced cell aggregation can be mediated by Gal-1.

It has been reported that in *N*-linked glycans, poly-LacNAc is added by  $\beta$ -1,3-*N*-acetylglucosaminyltransferase ( $\beta$ 3GNT) and  $\beta$ -1,4-galactosyltransferase ( $\beta$ 4GalT)<sup>23</sup>, after the branching process catalyzed by  $\beta$ -1,6-*N*-acetylglucosaminyltransferase V (GNT-V, encoded by *Mgat5*), and both GNT-V overexpression and poly-LacNAc structure are highly associated with cancer metastasis<sup>24, 25, 26</sup>. The interaction of Gal-3 to poly-LacNAc is thought to be involved in tumorigenic process<sup>27</sup>. Although Gal-1 and Gal-3 can interact with poly-LacNAc, Gal-1 prefers to bind terminal LacNAc residue<sup>28</sup> and Gal-3 prefers to internal LacNAc<sup>21</sup>. Terminal  $\alpha$ 2,3-sialylation or  $\alpha$ 1,2-fucosylation of poly-LacNAc was found to have no significant effect on Gal-1 or Gal-3 recognition of poly-LacNAc, while  $\alpha$ 1,3/4-fucosylation blocks Gal-1 and Gal-3 binding<sup>21, 29</sup>. In our study, we investigated extensively the *N*-glycan structures including sialylation, fucosylation and poly-LacNAc. Our results showed that the Gal-3BP expressed in more aggressive breast cancer cells MDA-MB-231 contained more poly-LacNAc structures and less sub-terminal  $\alpha$ 1,3/4-fucosylation comparing to the Gal-3BP from MCF-7. Therefore, the Gal-3BP derived from MDA-MB-231 has better binding ability to Gal-1 on cell surface and induces a higher level of cell aggregation.

Gal-3BP can self-assemble to form large oligomers, and according to the results from SEC-MALLS analysis (Fig. S7), Gal-3BP/MB231 formed larger oligomers (16-17 monomers) than Gal-3BP/MCF7 (12-13 monomers). In cell aggregation assay, we also observed that Gal-3BP/MB231 could induce larger cell aggregates, perhaps due to the interaction with cell surface Gal-1 to provide a higher degree of multivalent interaction between cells.

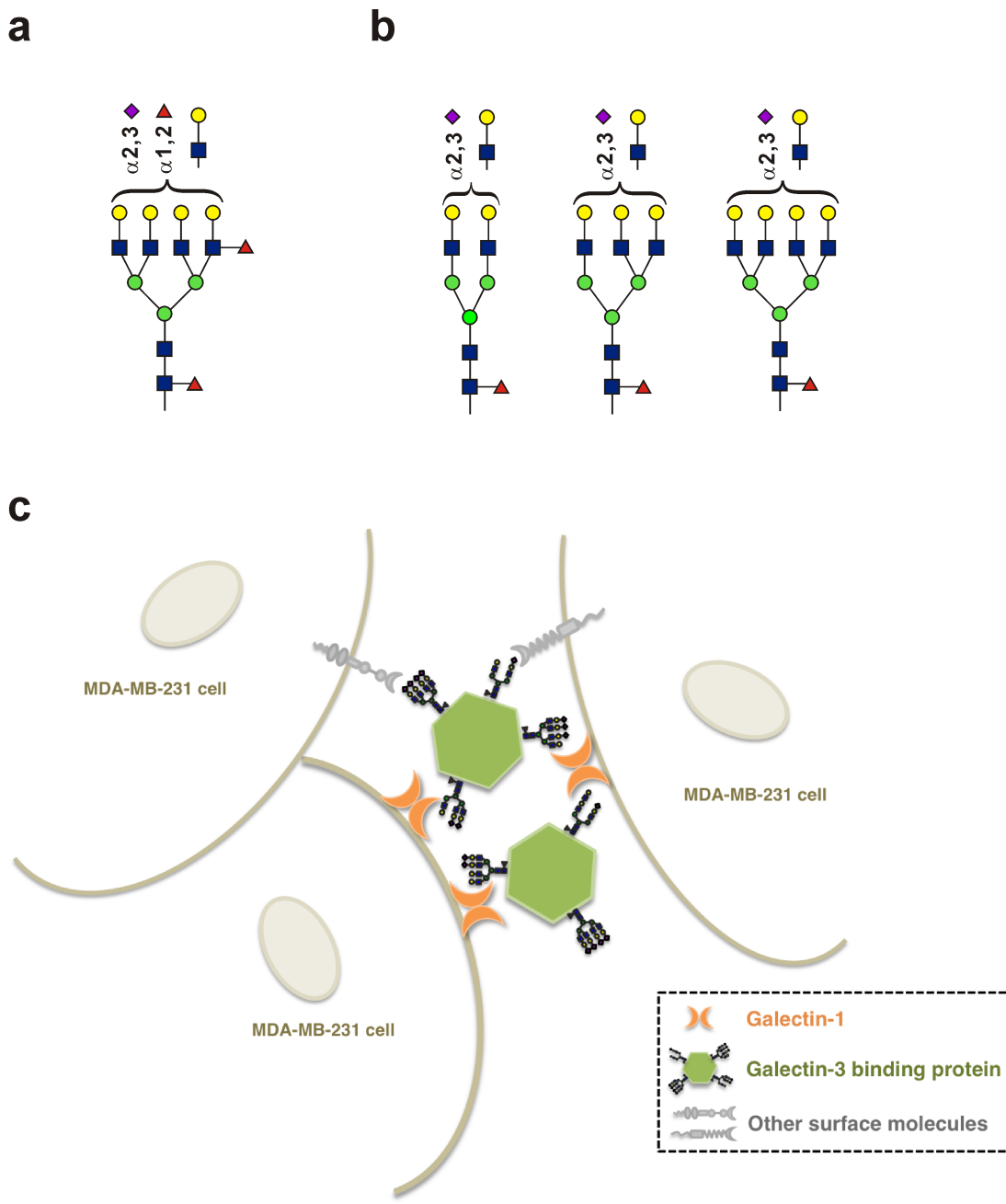


**Figure 5. The major glycoforms of Gal-3BP derived from MCF-7 cells (A) and MDA-MB-231 cells (B), and a hypothesized model of Gal-3BP-induced cell aggregation (C).**

In conclusion, we analyzed the detailed glycoforms of Gal-3BP/MCF7 and Gal-3BP/MB231 using LC-MS/MS and exoglycosidase treatment, and compared the differences in the *N*-linked glycan structures, including terminal sialylation,

fucosylation, branching and poly-LacNAc. The profiles of site-specific glycoforms of the proteins provide some information regarding their spatial orientation in modulating protein function and multivalent interaction (Fig.5). We further demonstrated that changes in Gal-3BP glycosylation can affect the binding for Gal-3 and Gal-1, the ability of Gal-3BP-mediated cell aggregation, and protein oligomerization, which can contribute to the metastatic potential of cancer.

## **ASSOCIATED CONTENT**

Supporting Information Available: Supplementary data and experimental procedures.

This information is available free of charge via the internet at <http://pubs.acs.org>.

## **AUTHOR INFORMATION**

Corresponding Author

chhwong@gate.sinica.edu.tw

Author Contributions

<sup>†</sup>T.-W.L. and H.-T.C. contributed equally to this work.

Notes

The authors declare no competing financial interests.

## **ACKNOWLEDGEMENTS**

We thank Dr. Fu-Tong Liu and Dr. Huan-Yuan Chen for providing various materials for galectin-related experiments and helpful discussion, Dr. Hsin-Yung Yen and Ms. Yu-Ling Chang for SEC-MALLS experiments, and the Academia Sinica Genomics Research Center MS Core Facilities for glycan analysis. This research was supported by the Genomics Research Center, Academia Sinica, Taiwan.

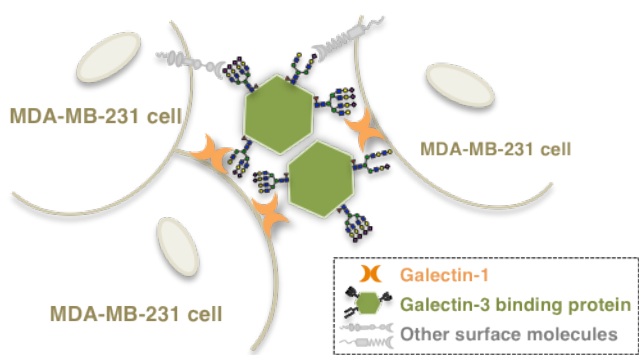
## References

- (1) Cazet, A.; Julien, S.; Bobowski, M.; Burchell, J.; Delannoy, P. *Breast Cancer Res* **2010**, *12*, 204.
- (2) Huang, Y. L.; Hung, J. T.; Cheung, S. K.; Lee, H. Y.; Chu, K. C.; Li, S. T.; Lin, Y. C.; Ren, C. T.; Cheng, T. J.; Hsu, T. L.; Yu, A. L.; Wu, C. Y.; Wong, C. H. *Proc Natl Acad Sci U S A* **2013**, *110*, 2517.
- (3) Varki, A.; Kannagi, R.; Toole, B. P. In *Essentials of Glycobiology*; Varki, A., Cummings, R. D., Esko, J. D., Freeze, H. H., Stanley, P., Bertozzi, C. R., Hart, G. W., Etzler, M. E., Eds.; The Consortium of Glycobiology Editors, La Jolla, California: Cold Spring Harbor NY, 2009.
- (4) Zhao, Y. Y.; Takahashi, M.; Gu, J. G.; Miyoshi, E.; Matsumoto, A.; Kitazume, S.; Taniguchi, N. *Cancer Sci* **2008**, *99*, 1304.
- (5) Bair, E. L.; Nagle, R. B.; Ulmer, T. A.; Laferte, S.; Bowden, G. T. *Prostate* **2006**, *66*, 283.
- (6) Grassadonia, A.; Tinari, N.; Iurisci, I.; Piccolo, E.; Cumashi, A.; Innominato, P.; D'Egidio, M.; Natoli, C.; Piantelli, M.; Iacobelli, S. *Glycoconj J* **2004**, *19*, 551.
- (7) Ozaki, Y.; Kontani, K.; Hanaoka, J.; Chano, T.; Teramoto, K.; Tezuka, N.; Sawai, S.; Fujino, S.; Yoshiki, T.; Okabe, H.; Ohkubo, I. *Cancer* **2002**, *95*, 1954.
- (8) Marchetti, A.; Tinari, N.; Buttitta, F.; Chella, A.; Angeletti, C. A.; Sacco, R.; Mucilli, F.; Ullrich, A.; Iacobelli, S. *Cancer Res* **2002**, *62*, 2535.
- (9) Kunzli, B. M.; Berberat, P. O.; Zhu, Z. W.; Martignoni, M.; Kleeff, J.; Tempia-Caliera, A. A.; Fukuda, M.; Zimmermann, A.; Friess, H.; Buchler, M. W. *Cancer* **2002**, *94*, 228.
- (10) Fusco, O.; Querzoli, P.; Nenci, I.; Natoli, C.; Brakebush, C.; Ullrich, A.; Iacobelli, S. *Int J Cancer* **1998**, *79*, 23.

- (11) Iacobelli, S.; Sismondi, P.; Giai, M.; D'Egidio, M.; Tinari, N.; Amatetti, C.; Di Stefano, P.; Natoli, C. *Br J Cancer* **1994**, *69*, 172.
- (12) Sasaki, T.; Brakebusch, C.; Engel, J.; Timpl, R. *EMBO J* **1998**, *17*, 1606.
- (13) Nonaka, M.; Ma, B. Y.; Imaeda, H.; Kawabe, K.; Kawasaki, N.; Hodohara, K.; Kawasaki, N.; Andoh, A.; Fujiyama, Y.; Kawasaki, T. *J Biol Chem* **2011**, *286*, 22403.
- (14) Shirure, V. S.; Reynolds, N. M.; Burdick, M. M. *PLoS One* **2012**, *7*, e44529.
- (15) Inohara, H.; Akahani, S.; Koths, K.; Raz, A. *Cancer Res* **1996**, *56*, 4530.
- (16) Ulmer, T. A.; Keeler, V.; Loh, L.; Chibbar, R.; Torlakovic, E.; Andre, S.; Gabius, H. J.; Laferte, S. *J Cell Biochem* **2006**, *98*, 1351.
- (17) Zhao, Q.; Barclay, M.; Hilkens, J.; Guo, X.; Barrow, H.; Rhodes, J. M.; Yu, L. G. *Mol Cancer* **2010**, *9*, 154.
- (18) Ozaki, Y.; Kontani, K.; Teramoto, K.; Fujita, T.; Tezuka, N.; Sawai, S.; Maeda, T.; Watanabe, H.; Fujino, S.; Asai, T.; Ohkubo, I. *Oncol Rep* **2004**, *12*, 1071.
- (19) Mbeunkui, F.; Metge, B. J.; Shevde, L. A.; Pannell, L. K. *J Proteome Res* **2007**, *6*, 2993.
- (20) Song, X.; Xia, B.; Stowell, S. R.; Lasanajak, Y.; Smith, D. F.; Cummings, R. D. *Chem Biol* **2009**, *16*, 36.
- (21) Stowell, S. R.; Arthur, C. M.; Mehta, P.; Slanina, K. A.; Blixt, O.; Leffler, H.; Smith, D. F.; Cummings, R. D. *J Biol Chem* **2008**, *283*, 10109.
- (22) Hirabayashi, J.; Hashidate, T.; Arata, Y.; Nishi, N.; Nakamura, T.; Hirashima, M.; Urashima, T.; Oka, T.; Futai, M.; Muller, W. E.; Yagi, F.; Kasai, K. *Biochim Biophys Acta* **2002**, *1572*, 232.
- (23) Lee, P. L.; Kohler, J. J.; Pfeffer, S. R. *Glycobiology* **2009**, *19*, 655.
- (24) Dennis, J. W.; Nabi, I. R.; Demetriou, M. *Cell* **2009**, *139*, 1229.
- (25) Granovsky, M.; Fata, J.; Pawling, J.; Muller, W. J.; Khokha, R.; Dennis, J. W. *Nature medicine* **2000**, *6*, 306.

- (26) Ito, N.; Imai, S.; Haga, S.; Nagaike, C.; Morimura, Y.; Hatake, K. *Histochemistry and cell biology* **1996**, *106*, 331.
- (27) Srinivasan, N.; Bane, S. M.; Ahire, S. D.; Ingle, A. D.; Kalraiya, R. D. *Glycoconjugate journal* **2009**, *26*, 445.
- (28) Di Virgilio, S.; Glushka, J.; Moremen, K.; Pierce, M. *Glycobiology* **1999**, *9*, 353.
- (29) Wai Wong, C.; Dye, D. E.; Coombe, D. R. *Int J Cell Biol* **2012**, *2012*, 340296.

## Table of Contents Graphic:



# **Galectin-3 binding protein and galectin-1 interaction in breast cancer cell aggregation and metastasis**

Tzu-Wen Lin<sup>†,‡</sup>, Hui-Tzu Chang<sup>†,§,¶</sup>, Chein-Hung Chen<sup>†</sup>, Chung-Hsuan Chen<sup>†</sup>,

Sheng-Wei Lin<sup>‡</sup>, Tsui-Ling Hsu<sup>†</sup> & Chi-Huey Wong<sup>†\*</sup>

<sup>†</sup>Genomics Research Center, Academia Sinica, 128 Academia Road, Section 2,  
Nankang, Taipei 115, Taiwan

<sup>§</sup>Institute of Biochemistry and Molecular Biology, National Yang-Ming University,  
Taipei 112, Taiwan

<sup>‡</sup>Institute of Biological Chemistry, Academia Sinica, 128 Academia Road, Section 2,  
Nankang, Taipei 115, Taiwan

## **Supplementary Information**

### **A. Supplementary Table and Figures**

### **B. Experimental Procedures**

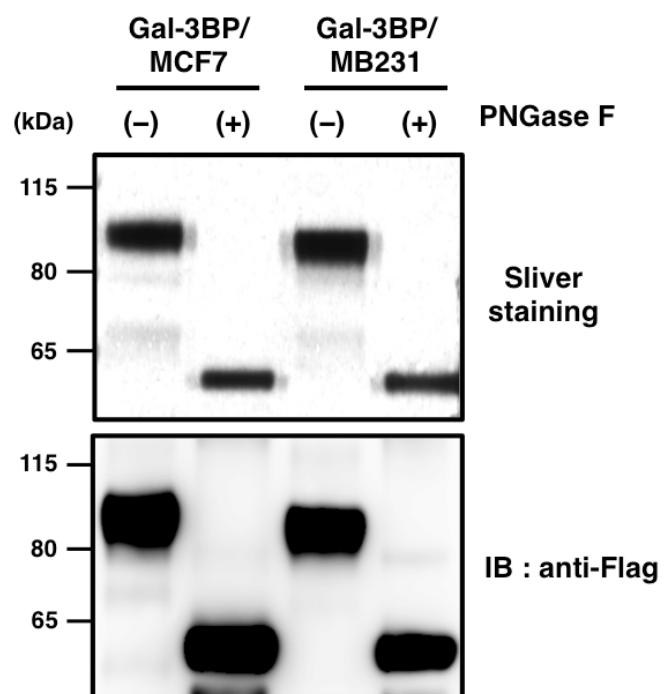


**Figure S1. PNGase F digestion of Gal-3BPs.** Purification of Gal-3BP-Flag secreted from MCF-7 and MDA-MB-231 cell culture supernatant. Gal-3BP-Flag protein was incubated with or without PNGase F and then examined by silver staining and immunoblotting with anti-Gal-3BP pAb.

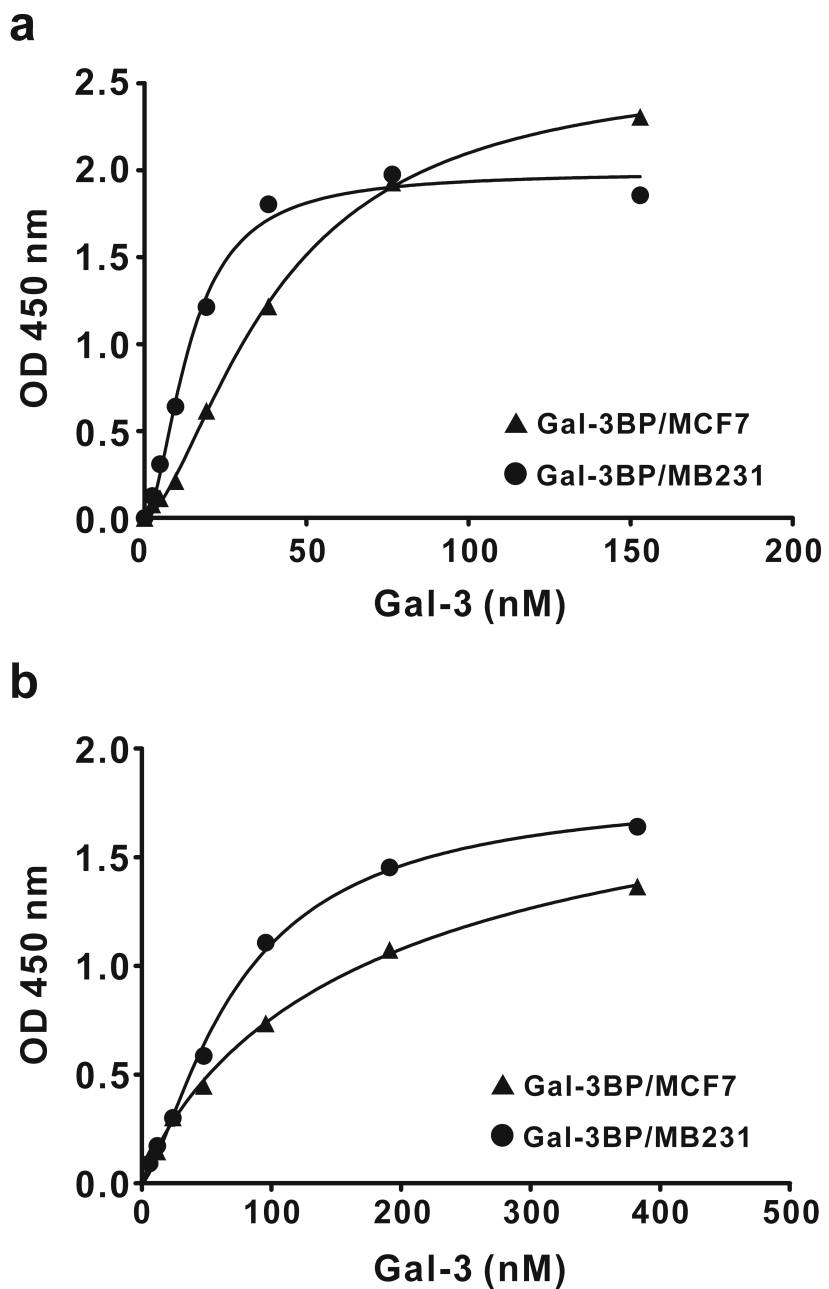


**Figure S2. Gal-3BP/MB231 has higher binding ability toward galectin (Gal)-3.**

Different concentrations of Gal-3 were applied to interact with immobilized (a) FLAG-tagged or (b) endogenous Gal-3BP/MCF7 or Gal-3BP/MB231 in microtiter plates, and bound Gal-3 was detected with biotinylated anti-Gal-3 antibody.

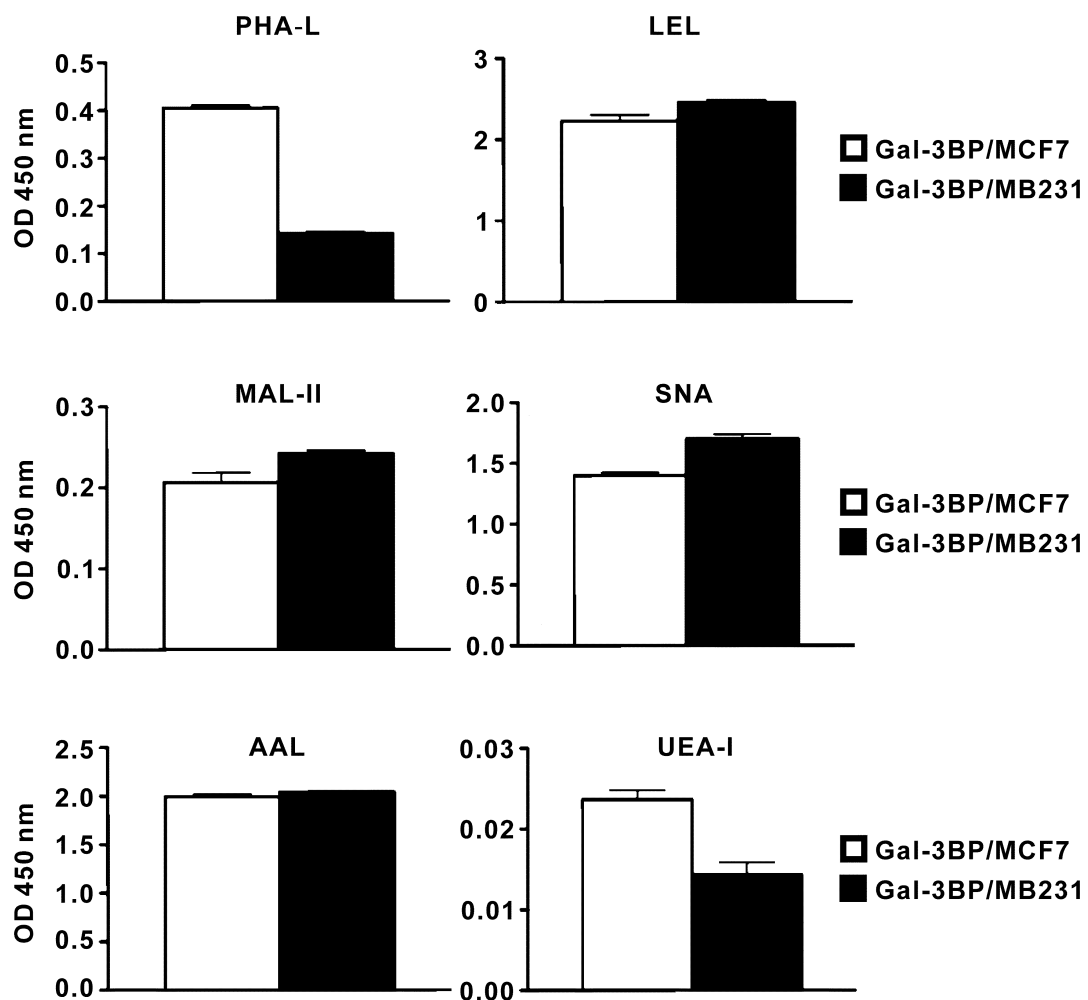


**Figure S3. Binding of Gal-3BP to lectins.** Specific binding of Gal-3BPs to lectins was measured by ELISA. Gal-3BP/MCF7 or Gal-3BP/MB231 (1  $\mu$ g/ml) was coated on wells and incubated with six kinds of biotinylated lectin (1  $\mu$ g/ml), PHA-L, LEL, MAL SNA, AAL, and UEA-1, individually. After washing, wells were incubated with streptavidin-HRP and then detected spectrophotometrically at OD<sub>450nm</sub>. Results are shown as mean  $\pm$  SD ( $n = 3$ ).

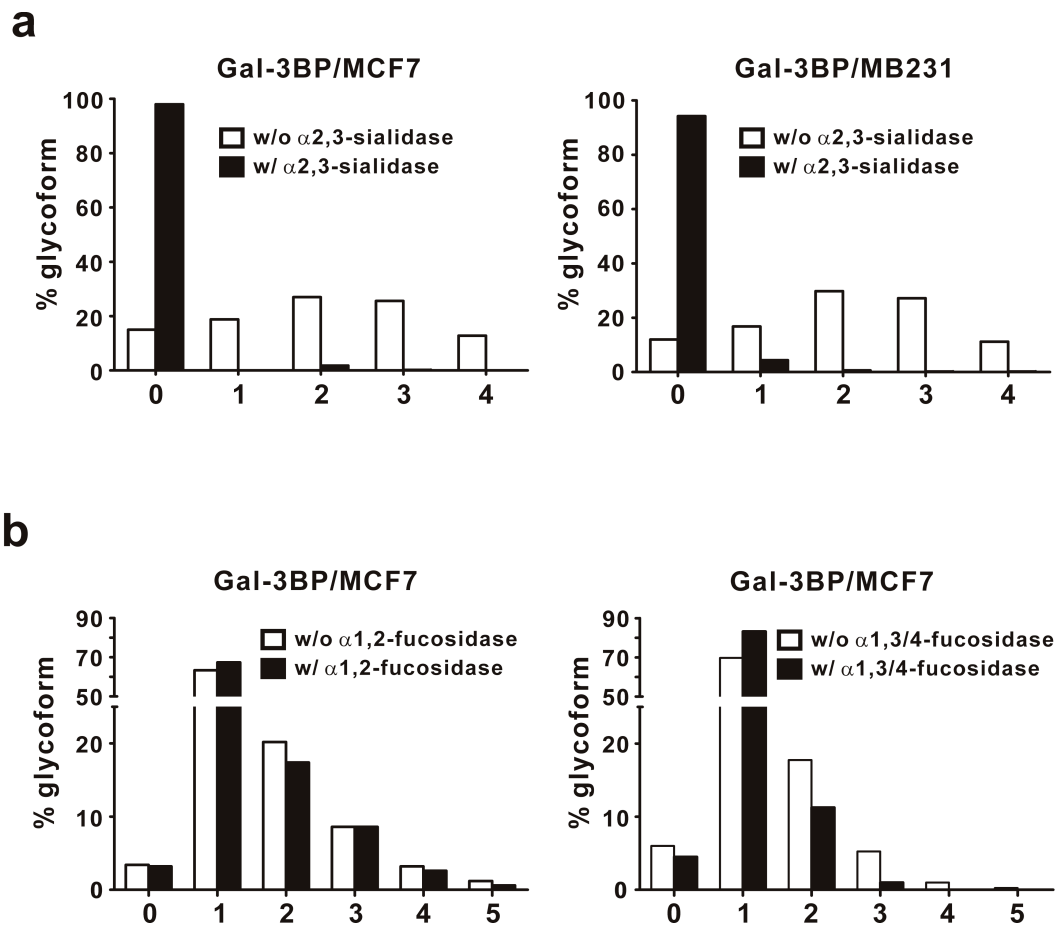


**Figure S4. Determination of sialic acid and fucose linkage of Gal-3BP.** (a) Distribution of sialic acid-containing glycoforms with or without  $\alpha$ 2,3-sialidase treatment. The glycoforms of Gal-3BP/MCF7 and Gal-3BP/MB231 are shown in the left and right panels, respectively. (b) Distribution of fucose-containing glycoforms with or without  $\alpha$ 1,2-fucosidase (left) or  $\alpha$ 1,3/4-fucosidase (right) treatment. The numbers of sialic acids (a) or fucoses (b) are indicated on the x-axis.

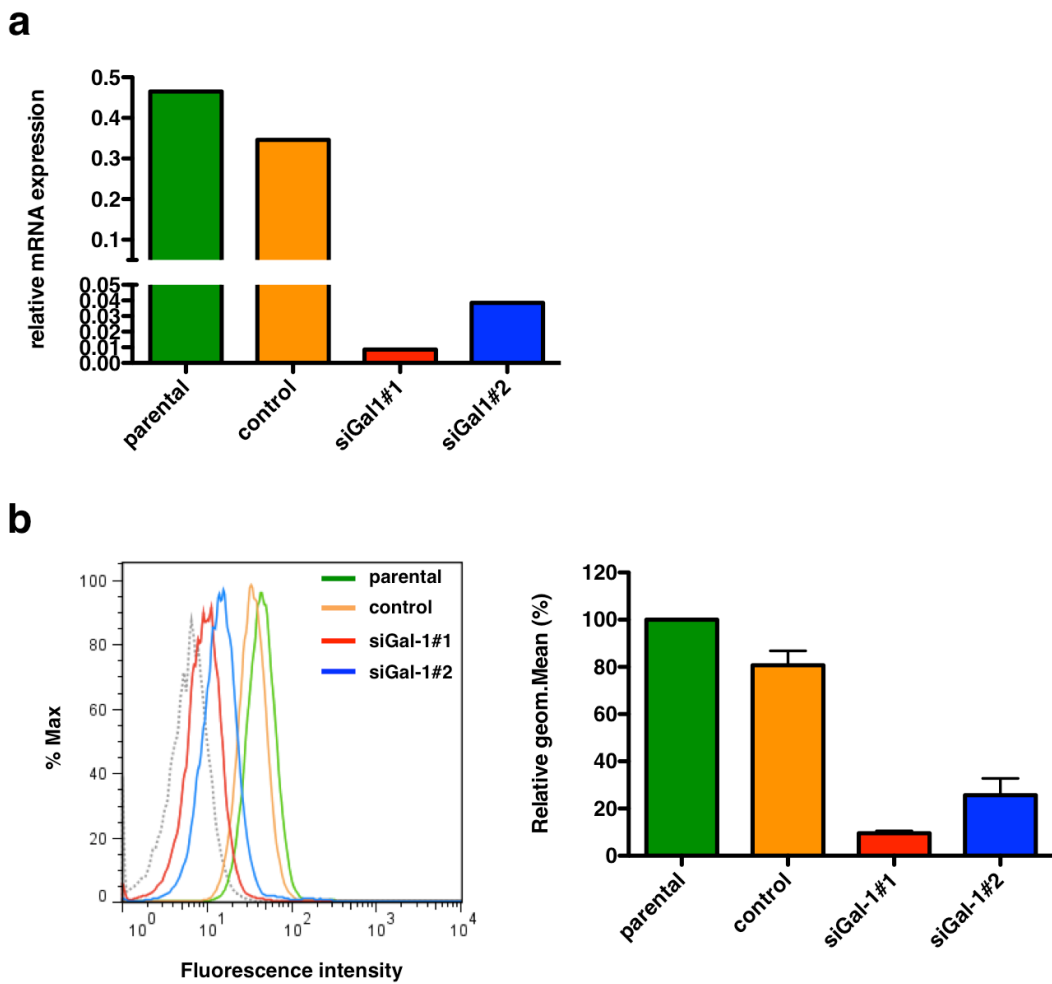


**Figure S5. Knockdown of Gal-1 expression in MDA-MB-231 cells** (a) Q-PCR analysis for Gal-1 mRNA expression was used to measure knockdown efficiency of isoform specific siRNA (siGal-1#1 and siGal-1#2) to Gal-1. The expression of Gal-1 was normalized against the expression level of GAPDH mRNA. (b) Flow-cytometric analysis of Gal-1 expression on MDA-MB-231 cells transfected with negative control or Gal-1 siRNA; the histogram on the right shows quantitative data. Green, parental cells; orange, negative control siRNA transfected cells; red, siGal-1#1 transfected cells; blue, siGal-1#2 transfected cells.

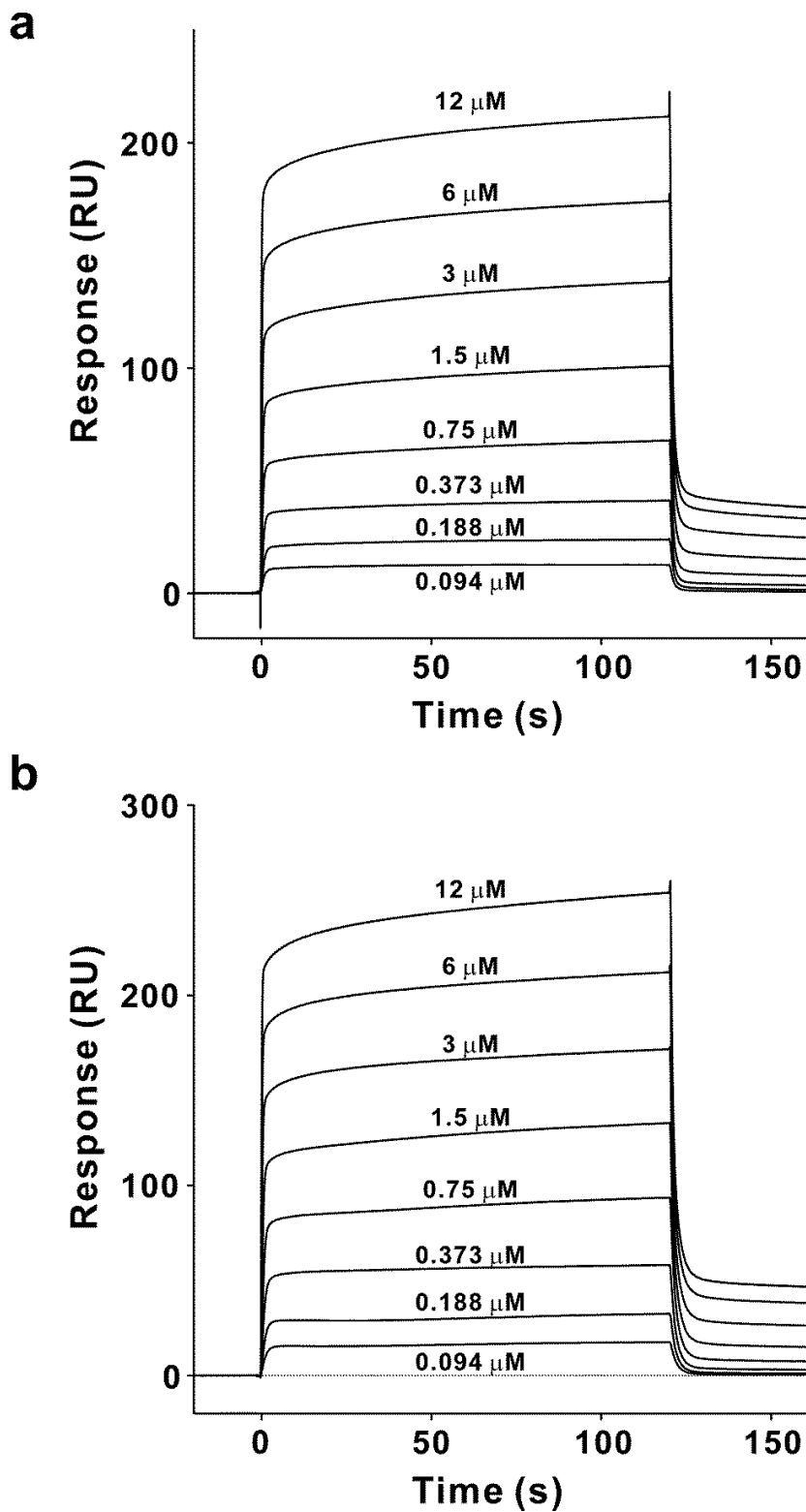


**Figure S6. Sensorgrams of Gal-1 binding to Gal-3BP.** Gal-3BP/MCF7 (a) and Gal-3BP/MB231 (b) were immobilized onto CM5 sensor chips as the ligand, and the concentrations of Gal-1 ranging from 0.094 to 12  $\mu\text{M}$  were injected as the analyte in the microfluidic channel to obtain RU.

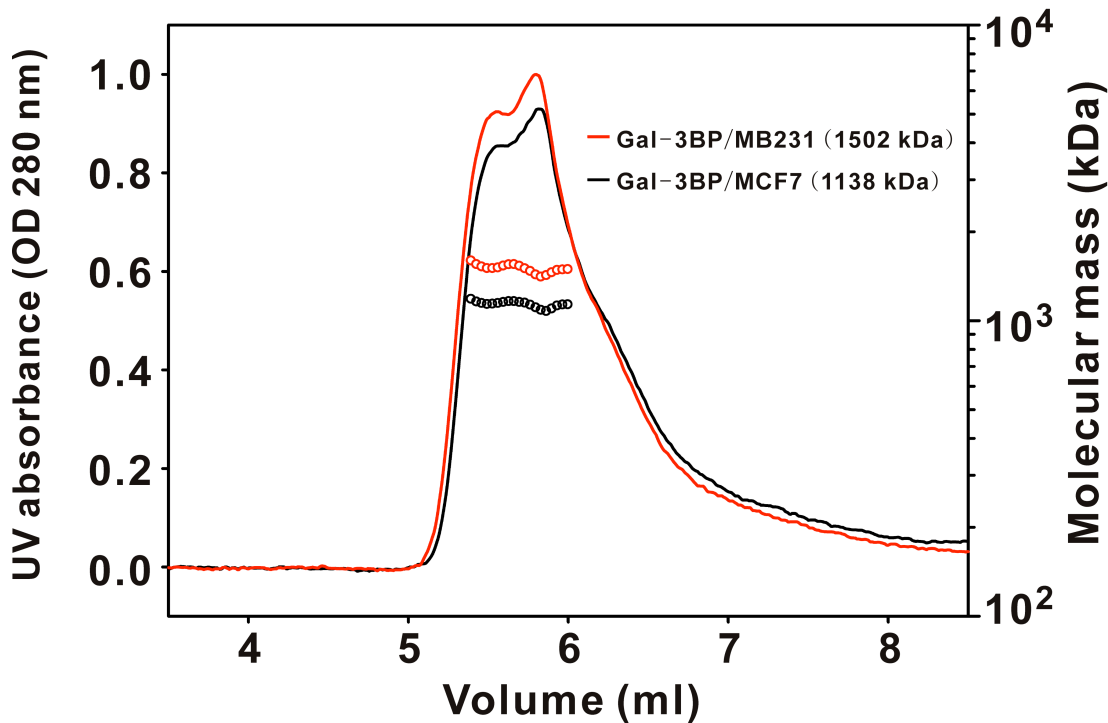


**Figure S7. Determination of the size of Gal-3BP/MCF7 and Gal-3BP/MB231 oligomers by HPLC size-exclusion chromatography multiangular laser light scattering (SEC-MALLS).** The chromatograms were obtained from SEC-MALLS measurements of native Gal-3BP/MCF7 (black) and Gal-3BP/MB231 (red) in PBS (pH 7.4). The solid lines represent the UV absorption, and the open circles correspond to the calculated molecular mass indicated on the right y-axis. The molecular mass of Gal-3BP oligomers was calculated by ASTRA software.

**Table S1.** Degalactosylated glycopeptide analysis in the MS/MS spectrum

	Gal-3BP/MCF7	Gal-3BP/MB231
	Number (Relative amount %)	Number (Relative amount %)
<b>Total glycopeptides/peptides</b>	51 (100%)	36 (100%)
Glycopeptides	48 (98.7%)	33 (97.6%)
Peptides	3 (1.35%)	3 (2.43%)
<b>Glycopeptides</b>	48 (100%)	33 (100%)
No fucose	5 (2.06%)	5 (1.65%)
1 fucose	29 (72.4%)	27 (97.8%)
2 fucose	6 (18.0%)	1 (0.53%)
3 fucose	8 (7.52%)	-
<b>Glycopeptides with 1 fucose</b>	29 (100%)	27 (100%)
{ (-) 512.2 oxonium ions	26 (95.4%)	26 (99.9%)
{ (+) 512.2 oxonium ions	3 (4.49%)	1 (0.04%)
{ (-) peptide+HexNAc+Fuc	14 (53.3%)	15 (56.8%)
{ (+) peptide+HexNAc+Fuc	15 (46.7%)	12 (43.2%)
<b>Glycopeptides with 2 fucoses</b>	6 (100%)	-
{ (-) 512.2 oxonium ions	1 (22.1%)	-
{ (+) 512.2 oxonium ions	5 (77.9%)	-
{ (-) peptide+HexNAc+Fuc	4 (75.4%)	-
{ (+) peptide+HexNAc+Fuc	2 (24.6%)	-
<b>Glycopeptides with 3 fucoses</b>	8 (100%)	-
{ (-) 512.2 oxonium ions	2 (32.0%)	-
{ (+) 512.2 oxonium ions	6 (68.0%)	-
{ (-) peptide+HexNAc+Fuc	5 (61.9%)	-
{ (+) peptide+HexNAc+Fuc	3 (38.1%)	-

## **Materials and Methods**

### **Cell culture**

MCF-7 (ATCC No. HTB-22) and MDA-MB-231 (ATCC No. HTB-26) cells are breast cancer cell lines. MCF-7 cells were grown in DMEM medium with 10% fetal bovine serum (FBS), 0.01 mg/ml recombined human insulin, and antibiotics at 37°C in 5% CO<sub>2</sub>. MDA-MB-231 cells were grown in Leibovitz's L-15 medium with 10% FBS, and antibiotics at 37°C in air.

### **Stable line establishment and purification of Gal-3BP-FLAG**

To establish human Gal-3BP stable clones, full-length cDNA that encodes human Gal-3BP was PCR amplified (forward primer: CCGGGCGGATCCGC CACCATGACCCCTCCGAGGCTC; reverse primer: GTAATCCTCGAGGTCCAC ACCTGAGGAGTTG), and inserted into BamHI/XhoI cut pFLAG-CMV-4a vector (Sigma-Aldrich) to obtain FLAG tag sequences. Gal-3BP-FLAG DNA was transfected into breast cancer cells using TransIT®-2020 transfection reagent (Mirus). Selection medium containing 750 µg/ml G418 after 48 h posttransfection, and selection was continued for 7-10 days to obtain cell populations containing Gal-3BP-FLAG. Stable clones were maintained in medium containing 500 µg/ml G418. To obtain human Gal-3BP-FLAG protein, conditioned medium was collected, centrifuged to remove cells, and filtered through 0.45 mm Millipore membrane. The resulting supernatant was applied to an anti-FLAG (M2) agarose (Sigma-Aldrich) column, after TBST (0.1% Tween-20) washing, Gal-3BP-FLAG was eluted by 0.1 M Glycine HCl (pH 2.5), and then neutralized by 1M Tris-HCl (pH 9.0). The eluted Gal-3BP-FLAG was buffer exchanged to PBS and stored at -80°C. The purity of protein was checked by SDS-PAGE with silver (Thermo) staining.

### **Binding ability of Gal-3BP and Gals**

Gal-3BPs (0.1 µg in 100 µL of 100 mM sodium carbonate buffer, pH 9.6) purified from breast cancer cells MCF-7 or MDA-MB-231 were coated in each well of 96-well microtiter plates at 4°C overnight. Wells were washed with 300 µL PBST (PBS with 0.05% (v/v) Tween 20, pH 7.4) three times, and then blocked with 300 µL of 1 × Carbo-Free blocking solution (Vector Labs) for 2 h at room temperature. Various concentrations of Gal-3 (R&D Systems) or Gal-1 in PBST were added into the wells coated with or without Gal-3BP and incubated at 37°C for 1 h. After binding, wells were washed five times with PBST and further incubated with 100 µL of 1 mg/mL biotinylated anti-Gal-3 MAb (M3/38) or biotinylated anti-Gal-1 polyclonal Ab (1:2000 in PBST) in PBST at 37°C for 1 h. Wells were then washed and incubated with 100 µL of peroxidase-conjugated streptavidin (1:2500 in PBST) at room temperature for 1 h. After washing the plate five times, 100 µL of 3,3',5,5'-tetramethylbenzidine (TMB) solution (Invitrogen) was added to the wells and the reaction was developed at room temperature for 10 min. 2 N H<sub>2</sub>SO<sub>4</sub> (100 µL) was then added to each well to stop the reaction, and the plate was read at OD450. Another setting was to immobilize Gal-1 (0.5 µg in 100 µL of 100 mM sodium carbonate buffer, pH 9.6) in each well of 96-well microtiter plates and the experimental procedures were similar to those described above. In brief, after blocking, various concentrations of Gal-3BPs from MCF7 or MDA-MB-231 cells in PBST were added into wells and the plates were incubated at 37°C for 30 min. Following washing, HRP-conjugated anti-Gal-3BP antibody (eBioscience) was added into wells and the plates were incubated at 37°C for 45 min. After washing the plate five times, 100 µL of TMB solution was added into the wells and the reaction was developed at room temperature for 10 min.

## **In-solution trypic digestion of protein samples and treatment with exoglycosidases**

FLAG-tagged Gal-3BP samples (5 µg in 30 µL) were diluted in buffer with 50 mM NH<sub>4</sub>HCO<sub>3</sub> and 0.1% RapiGest (Waters), and subjected to reduction with 5 mM DTT and alkylation with 15 mM iodoacetamide. After quenching with 5 mM DTT, 0.5 µg trypsin was added and the mixture was incubated at 37°C overnight, followed by heat-inactivation of trypsin at 95°C for 10 min. When samples cooled down, trifluoroacetic acid was added (final 0.5%) and the samples were further incubated at 37°C for 45 min to crash RapiGest. Insoluble hydrolyzed RapiGest was removed by centrifuge at 14,000 rpm for 15 min, and the supernatant was dried using a SpeedVac concentrator. Desialylation of trypsin-digested Gal-3BP was performed by treating with 0.1% formic acid at 80°C for 1 h. To detect the linkages of sialic acid or fucose, Gal-3BP glycopeptide samples were treated with α2,3-sialidase (Prozyme) or fucosidases (α1,2-fucosidase and α1,3/4-fucosidase (Prozyme)), respectively, at 37°C overnight in a 20 µl reaction under the conditions suggested by the vender. For degalactosylation, desialylated glycopeptides were further incubated with β1,3/4-galactosidase (Prozyme) at 37°C overnight with the buffer suggested by the vender.

## **Analysis of glycopeptides using LC-MS/MS**

The glycopeptides with or without exoglycosidase treatment were analyzed by high resolution and high mass accuracy nanoflow LC-MS/MS. Glycopeptide samples were injected at 10 µL/min into a precolumn (150 µm I.D. × 30 mm, 5 µm, 200 Å) and then separated in a reversed phase C18 nano-column (75 µm I.D. × 200 mm, 3 µm, 200 Å) for analysis in an LTQ Orbitrap XL ETD mass spectrometer (Thermo Fisher

Scientific) equipped with a nanoelectrospray ion source (New Objective). Separation was performed at 300 nL/min using 0.1% formic acid in water as mobile phase A and 0.1% formic acid in 80% acetonitrile as mobile phase B. Survey full scan MS spectra (from m/z 320 to 2000) were acquired in the orbitrap with a mass resolution of 30,000 at m/z 400. The three most intense ions were sequentially isolated for HCD (Resolution 7500) and the electrospray voltage was maintained at 1.8 kV with the capillary temperature set at 200°C. The MS spectra were acquired for compositional assignment and quantitation of glycopeptides. Assignment of glycopeptides was based on matching the measured masses with the database, which combined predicted masses of tryptic peptides (by Protein Digest Simulator Basic) and *N*- and *O*-linked glycans (from the Consortium of Functional Glycomics), as well as the retention time of the glycopeptides by in-house software. Each assigned glycopeptide was confirmed by the appearance of glycan fragments in its MS/MS spectra.

### **Lectin-based ELISA**

Ninety-six-well ELISA plates (Bio-Rad) were coated with 100 μL of affinity-purified Gal3BP-FLAG (5 μg/ml) from MCF-7 or MDA-MB-231 cells for 1 h, and blocked with Carbo-free blocking buffer for 4 h at room temperature. Plates were then washed (four times) with washing buffer (PBS with 0.1% Tween 20). Different biotinylated lectins (100 μL) were added at a concentration of 1 μg/ml in washing buffer and incubated for 2 h at room temperature. The lectins were detected with a streptavidin-conjugated horseradish peroxidase. The lectins used include PHA-L, LEL, MAL, SNA, AAL, UEA-1 and LTL. The binding signal was detected spectrophotometrically at 450 nm.

### **Cell aggregation**

Breast cancer cells were harvested with 0.02% EDTA in PBS, and single-cell suspensions ( $1 \times 10^6$  cells/mL in PBS) were incubated with Gal-3BP with or without 10 mM lactose or sucrose. Aliquots containing 0.5 mL of the cell suspension were placed in BD falcon round-bottom tubes and agitated at 100 rpm at 37°C for up to 1 h. Aggregation was stopped by fixing the cells with 2% paraformaldehyde. Snapshots were taken of cells and the degree of cell aggregation was analysed by Image J.

### **Immunofluorescence staining**

Breast cancer cell samples treated with or without Gal-3BP were incubated with anti-Gal-3BP Ab (10 µg/mL, R&D Systems) for 30 min at 4°C, washed twice with PBS, and incubated with PE-conjugated anti-goat IgG Ab (2.5 µg/ml, R&D Systems) for 30 min at 4°C. After washing, the cells were mounted on slides with Hoechst 33343 for fluorescence microscopy.

### **Quantitative-PCR**

Total mRNAs were extracted using RNeasy Mini kit (Qiagen). Two micrograms of total RNAs was reverse-transcribed to generate cDNA by a High-Capacity cDNA Reverse Transcription kit (Life Technologies). Quantitative-PCR (Q-PCR) was performed using FastStart TagMan Probe Master kit (Roche) according to the manufacturer's instructions and analyzed on an ABI 7300 Real-Time PCR system. The relative expression levels of galectins were normalized with GAPDH mRNA. Primers and probes for all the galectins detected in this study were kindly provided by Dr. Fu-Tong Liu.

### **Flow cytometry**

Breast cancer cells were suspended at a concentration of  $1 \times 10^7$  cells/mL in FACS buffer (PBS supplemented with 1% FBS and 0.1% sodium azide). Cells were stained with 10 µg/mL of rabbit polyclonal antibodies against galectin-1, -3, -8, or -9 for 30 min on ice. After washing with FACS buffer and incubation with FITC-conjugated secondary antibody for 30 min on ice in the dark, the cells were analyzed by flow cytometry using FACSCanto (BD Biosciences).

### **Gal-1 knockdown experiments**

Two siRNA sequences against Gal-1: siGal-1 (#s8146) and siGal-2 (#s194592) were purchased from Life Technologies. Transfection of siRNAs was performed with Lipofectamine RNAiMAX reagent (Life Technologies) according to the manufacturer's instructions. Knockdown efficiency was determined by quantitative RT-PCR (Q-PCR).

### **Surface plasmon resonance (SPR) of Gal-1 binding to immobilized Gal-3BP.**

SPR experiments were performed on a Biacore T200 instrument (Biacore GE Healthcare) at 25 °C in HBS-EP+ buffer (10 mM Hepes, pH 7.4, 150 mM NaCl, 3.4 mM EDTA, 0.0005% surfactant P20) as running buffer. Two kinds of Gal-3BP (Gal-3BP/MCF7 and Gal-3BP/MB231) were immobilized on CM5 sensor chips, by amine coupling, according to the manufacturer's instruction. Gal-3BPs were diluted at 10 µg/ml in coupling buffer (10 mM acetate, pH 4.5) and injected until the desired immobilization level was reached (~600 Resonance Units RU). Solutions of different concentrations of Gal-1 (12, 6, 3, 1.5, 0.75, 0.375, 0.188 and 0.094 µM) in running buffer were injected for 2 min at a flow rate of 30 µl/min through Gal-3BP coated

channels. Bound Gal-1 was eluted with running buffer and the chips were regenerated with 0.1 M lactose in PBS. Sensorgrams of each Gal-3BP were superimposed, and the steady-state isotherms and the  $K_D$  values were obtained using the fitting tool of the Biacore T200 Evaluation software version 2.0 (BIAcore).

### **Size-exclusion chromatography-multi-angle laser light scattering**

Size-exclusion chromatography-multi-angle laser light scattering (SEC-MALLS) was performed using Shodex protein KW-803 HPLC column ( $30 \times 0.8$  mm) in PBS buffer (pH 7.4). For each round of Gal-3BP sample, 5  $\mu$ g of Gal-3BP was injected into HPLC apparatus (Agilent 1260 series LC system) at a flow rate of 0.5 mL/min at room temperature and monitored by UV-visible detector (280 nm). Intensities of light scattering were measured using a DAWN-HELEOS detector (Wyatt Technology). Astra software version 5.3.4.20 (Wyatt Technology) was used to analyze the light scattering data.